Martin 64B

Massachusetts Institute of Technology
Instrumentation Laboratory
Cambridge, Massachusetts

Space Guidance Analysis Memo # 15-67

TO: SGA Distribution

FROM: Edward Womble

DATE: September 8, 1967

SUBJECT: Preliminary Design of the RCS Autopilots Required for Task 2 of the Apollo Application Program

Introduction

One phase of the Apollo Applications Program entails the rendezvous of a CSM/LM-ATM vehicle with an OWS. The rendezvous will be accomplished by placing the CSM/LM-ATM in several steps until the rendezvous is completed. Due to visual and radar considerations, the z axis of the LM (which is the primary vehicle) will be aligned with the velocity vector. Mission requirements call for a maximum deceleration along the z axis, necessitating the use of RCS jets on both the CSM and LM.

The CSM/LM-ATM configuration will be different from the Apollo CSM/LM configuration, in that the z and y body axes of the LM will be parallel to the z and y control axes of the CSM. The new alignment creates a slight problem due to the fact that jets # 3, 4, 7, and 8 on the CSM, and # 1, 5, 9, and 13 on the LM must be inhibited from firing. This is due to the plume impingement of these jets on the windows and antennas.

In order to accomplish the mission goals, subject to the new constraints, two new autopilot concepts are required. Before the attitude autopilot concepts are discussed, the pitch, roll, and yaw axes must be defined for the new vehicle configuration. The axes are defined with respect to the LM pilot in the LM body coordinate system and are shown in Fig. 1.

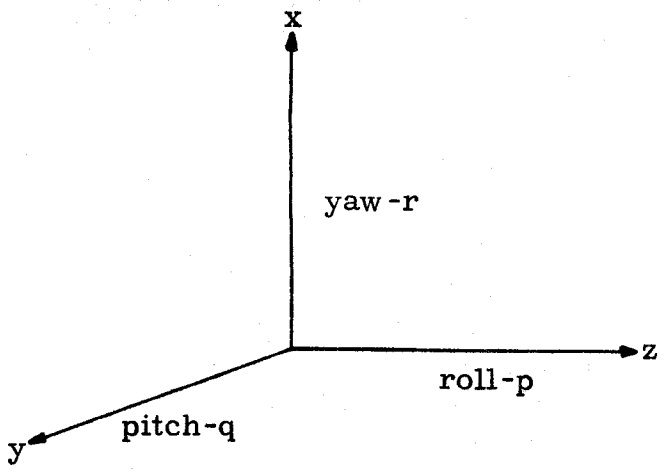

Figure 1 Definition of the Rotations

One autopilot concept will be required to control pitch during a z axis translation firing and roll during a y axis translation firing. The objective during these two types of firing will be either maximum acceleration or deceleration; therefore, translational jets on both the CSM and the LM must be fired. This means that one computer (either LGC or CMC) must contain the logic for controlling both sets of jets, and that commands must be transmitted between the LGC and the CMC via a crosslink. The second autopilot concept will be required to perform attitude hold and attitude maneuvers without the inhibited jets.

The preliminary design of these two type of autopilots follows.

Translation Attitude Hold Autopilots

In order to produce maximum acceleration and deceleration during either a z axis or a y axis firing, the control must be such that the jets, along the desired translation axis, of both the CSM and LM are fired. Since the moment arm of the CSM is considerably larger than the moment arm of the LM, the obvious maximum acceleration control is to continuously fire the LM jets and pulse width modulate the CSM jets to obtain the necessary attitude control (pitch during a z axis firing and roll during a y axis firing). A convenient method for generating the pulse width modulating control is to choose the desired limit cycle in the phase plane, and then adjust the phase plane logic so that the desired limit cycle is the only limit cycle and is stable. It will be assumed that the vehicle can be represented as a rigid body and that the body angular rates are low enough (each DAP will be in the attitude hold mode) so that the axes are uncoupled. With these assumptions, the differential equation for pitch during a minus z axis firing becomes

$$\ddot{q} = (F\ell_{CSM}/I_{yy})\, u_{CSM} - (F\ell_{LM}/I_{yy})\, u_{LM}\,;\ \left.\begin{matrix} u_{CSM} \\ u_{LM} \end{matrix}\right\} = -1,\ 0,\ +1\,. \tag{1}$$

When only the LM jets are fired, (1) becomes:

$$\ddot{q} = -(F\ell_{LM}/I_{yy}) = -K_L\,. \tag{2}$$

The solution of (2) is

$$q = -\dot{q}^2/2K_L + (q_0 + \dot{q}_0^2/2K_L)\,. \tag{3}$$

Equation (3) defines a family of parabolas symmetrical about the q axis and opening to the left. When both the CSM and the LM jets are fired, (1) becomes

$$\ddot{q} = (\ell_{CSM} - \ell_{LM})\, F/I_{yy} = K_{LC}\,. \tag{4}$$

The solution of (4) is

$$q = \dot{q}^2/2K_{LC} + (q_0 - \dot{q}_0^2/2K_{LC}). \tag{5}$$

Equation (5) defines a family of parabolas symmetrical about the q axis and opening to the right.

The Hamel Locus approach can be used to find the locus of points such that if the CSM jets are switched from one mode to the other at any point along the locus, the rigid body vehicle will support a limit cycle which will pass through that point. Let the initial pitch angle and pitch rate be q_0 and $\dot{q}_0$, and let the CSM jets be off. The vehicle will follow the state space trajectory defined by (3) until the CSM jets are turned on. Let the pitch angle and pitch rate be γ and $\dot{\gamma}$ when the CSM jets are turned on. The vehicle will then follow the state space trajectory defined by (5) until the CSM jets are turned off. Let the pitch angle and pitch rate be ϵ and $\dot{\epsilon}$ when the CSM jets are turned off. The conditions for a limit cycle are $\epsilon = q_0$ and $\dot{\epsilon} = \dot{q}_0$, where

$$\epsilon = \dot{\epsilon}^2/2K_{LC} + (\gamma - \dot{\gamma}^2/2K_{LC}) \tag{6}$$

and

$$\gamma = -\dot{\gamma}^2/2K_L + (q_0 + \dot{q}_0^2/2K_L). \tag{7}$$

Letting $\epsilon = q_0$ and $\dot{\epsilon} = \dot{q}_0$ in (6) yields:

$$q_0 = \dot{q}_0^2/2K_{LC} + (\gamma - \dot{\gamma}^2/2K_{LC}),$$

or,

$$\gamma = \dot{\gamma}^2/2K_{LC} + (q_0 - \dot{q}_0^2/2K_{LC}). \tag{8}$$

Equating the right hand sides of (7) and (8) yields:

$$\dot{\gamma}^2/2K_{LC} + q_0 - \dot{q}_0^2/2K_{LC} = -\dot{\gamma}^2/2K_L + q_0 + \dot{q}_0^2/2K_L,$$

or,

$$|\dot{\gamma}| = |\dot{q}_0| \tag{9}$$

Due to the fact that the trajectories are parabolas symmetrical about the q axis, (9) means that the magnitude of the rates at the switch points must be equal and the switch points must lie on one of an infinite number of lines which are parallel to the q axis. The phase plane logic will now be determined so that the only points where the switch from CSM jets on to off and vice versa can occur, with equal magnitudes of rates and equal angles, lie on the desired limit cycle. Consider the switch curve shown in Fig. 2 by the solid line. The parabolic portion of the switch curve is from (3),

$$q = -\dot{q}^2/2K_L + q_{LM}\,, \tag{10}$$

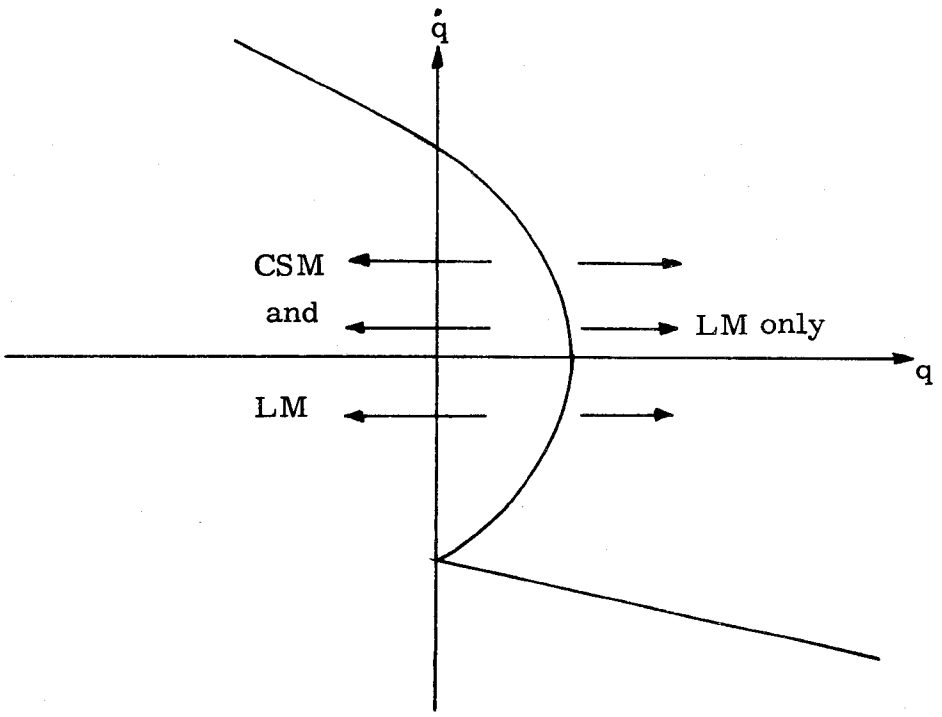

Figure 2 Proposed Translation Attitude Hold Autopilot

where q_{LM} is the maximum allowable pitch error during the time that the CSM jets are off. The straight line portion of the curve is a tangent to the desired limit cycle at q = 0. The equation of the line is found from the equation of the desired limit cycle when both the CSM and the LM jets are fired.

$$q = \dot{q}^2/2K_{LC} - q_{LC} , \tag{11}$$

where q_{LC} is the maximum allowable pitch attitude error. Differentiating q as given by (11) with respect to $\dot{q}$ yields:

$$d\,q/\,d\,\dot{q} = \dot{q}/K_{LC}$$

Therefore, the equation of the straight line section of the switch curve is

$$q = -\,\dot{q}\,\dot{q}_{max}/K_{LC} - \dot{q}^2_{max}/K_{LC}, \tag{12}$$

where q_{max} is the maximum allowable rate during the limit cycle.

Due to the facts that the trajectories in the phase planes are parabolas, the switch curve has a negative slope and a positive q axis intercept in the second quadrant, and the switch curve has a negative slope and a negative q axis intercept in the fourth quadrant, the system is asymptotically stable in the region of the phase plane which is outside of the desired limit cycle. In order to justify this statement consider Fig. 3.

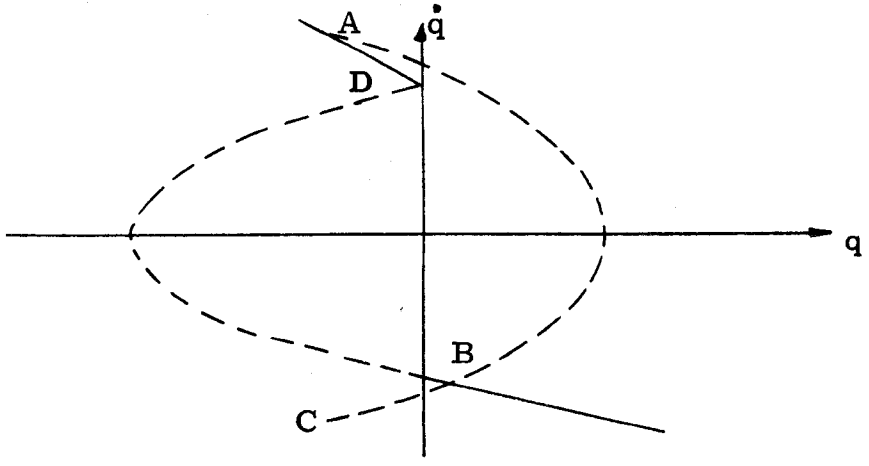

Figure 3 A Typical Trajectory Starting in Quadrant Two and Switching in Quardrant 4

The magnitude of the velocity at point B is less than the magnitude at point A, because the trajectory would have to get to point C before the magnitude of the velocity would be equal to its magnitude at point A. Therefore, the trajectory is converging to the desired limit cycle. Similarly, the magnitude of the velocity at point D is less than its magnitude at point B; therefore, when the state of the vehicle is outside the desired limit cycle the system is asymptotically stable. When the state of the vehicle is inside the desired limit cycle the system is unstable; therefore, besides being the only limit cycle, the desired limit cycle is also a stable limit cycle.

The effects of sampling will be to shift the switch curve so that other possible limit cycles exist, as is shown in Fig. 4. However, the limit cycle caused by sampling will have no effect on the performance of the system for its intended mission. Therefore, the firing times of the jets for this mode of operation will <u>not</u> have to be calculated.

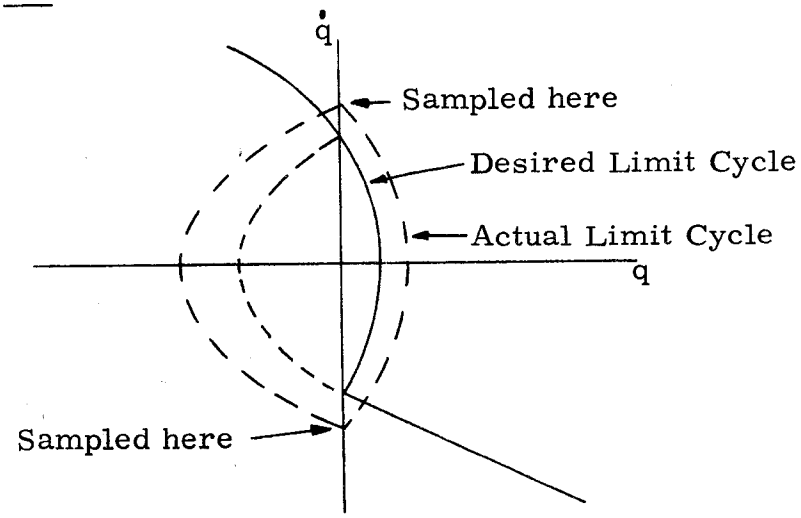

Figure 4 An Example of the Effects of Sampling

A second source of error is the uncertainty in the actual values of K_{LC} and K_L. The uncertainty in the value of K_{LC} will not effect the performance of the system, because it will only change the shape of the desired limit cycle. This is illustrated in Fig. 5. However, the effects of the uncertainty of the value of K_L will be much more severe. When K_L is much larger than its nominal value, chattering of the CSM jets will result, as is shown in Fig. 6. However, the desired limit cycle will still be obtained, and the fuel penalty does not appear to be severe because the additional firings of the CSM jets

will result in a greater translation deceleration force. When K_L is lower than its nominal value, an infinite number of limit cycles exist between $\dot{q}_{max}$ and $-\dot{q}_{max}$. These limit cycles are illustrated in Fig. 7. Again the CSM jets will be fired more often than for the nominal case, which will result in a greater translation deceleration force being produced.

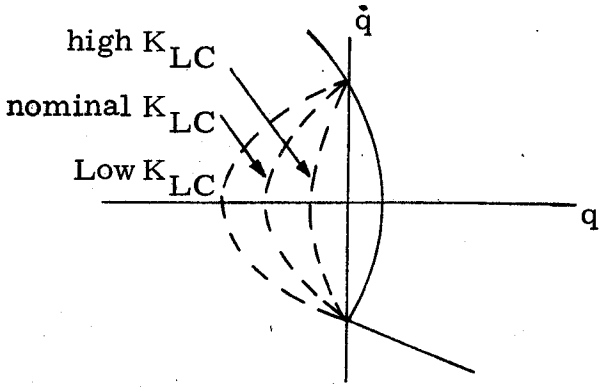

Figure 5 The Effects of the Uncertainty of the Value of K_{LC}

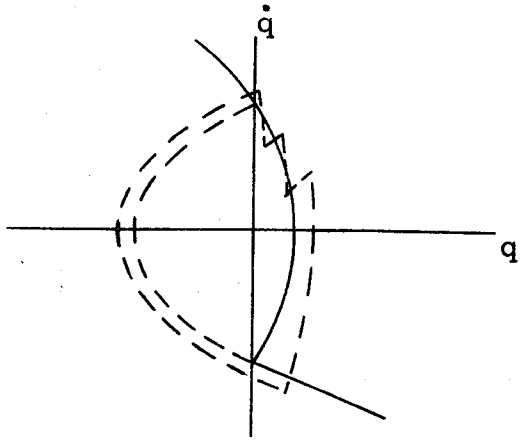

Figure 6 An Illustration of the Effects of K_L being much Larger than Expected

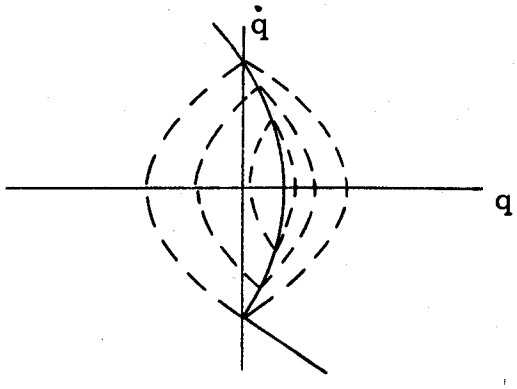

Figure 7 The Effects of K_L being much Smaller than Expected

The variations in K_L do not appear to be a problem at first glance; however, a problem of exciting either bending or sloshing resonances might develop due to either the chattering (K_L high) or the possible frequencies of the limit cycle (K_L low). If this problem does develop, the system can easily be made adaptive. One adaptive procedure will be listed below.

Both q_{LM} and q_{max} are functions of q_{LC}. The relationship between q_{max} and q_{LC} can be derived from (11) due to the fact that when $q = 0$, $q = q_{max}$. Therefore,

$$q_{max} = \sqrt{2 K_{LC} q_{LC}} \quad , \tag{13}$$

When the vehicle is in the desired limit cycle and following the trajectory given by (11), $q = 0$ when $q = \dot{q}_{max}$; therefore,

$$q_{LM} = \dot{q}^2_{max} / 2 K_L . \tag{14}$$

Substituting (13) into (14) yields:

$$q_{LM} = (K_{LC}/K_L)\, q_{LC} \tag{15}$$

Therefore, the adaptive procedure is:

(1) Read in the maximum allowable pitch attitude error (q_{LC})

(2) If the CSM jets are turned off and then on without $\dot{q}$ changing signs:

(a) Increase K_L by a prespecified fixed percentage, and recalculate q_{LM} using (15).

$$q_{LM} = (K_{LC}/K_L)\, q_{LC} \tag{15}$$

(b) Update the parabolic portion of the switch curve using (10).

$$q = -\dot{q}^2/2K_L + q_{LM} \tag{10}$$

(3) If the CSM jets are switched off and then on, as $\dot{q}$ goes from $+\dot{q}_0$ to $-\dot{q}_0$, in less than a prespecified number of samples, n:

(a) Recalculate K_L using:

$$K_L = 2\dot{q}_0/nT, \tag{16}$$

where T is the sample period.

(b) Recalculate q_{LM} using (15).

$$q_{LM} = (K_{LC}/K_L)\, q_{LC} \tag{15}$$

(c) Update the parabolic portion of the switch curve using (10).

$$q = -\dot{q}^2/2K_L \tag{10}$$

The adaptive system will not be used unless further studies indicate that problems due to the excitation of vehicle resonances exist.

When the positive z axis jets are fired, the phase plane trajectories are simply rotated 180^o; therefore, the autopilot given in Fig. 2 can also be used for + z axis firings. All that is necessary is that - q and $-\dot{q}$ be fed into the autopilot, and the control be multiplied by - 1.

Flowcharts of the proposed pitch and roll translation attitude hold autopilots are given in Figs. 8 and 9. Note that the only difference between the two autopilots is that the CSM jets generate a positive pitch moment during a - z axis firing and a negative roll moment during a - y axis firing.

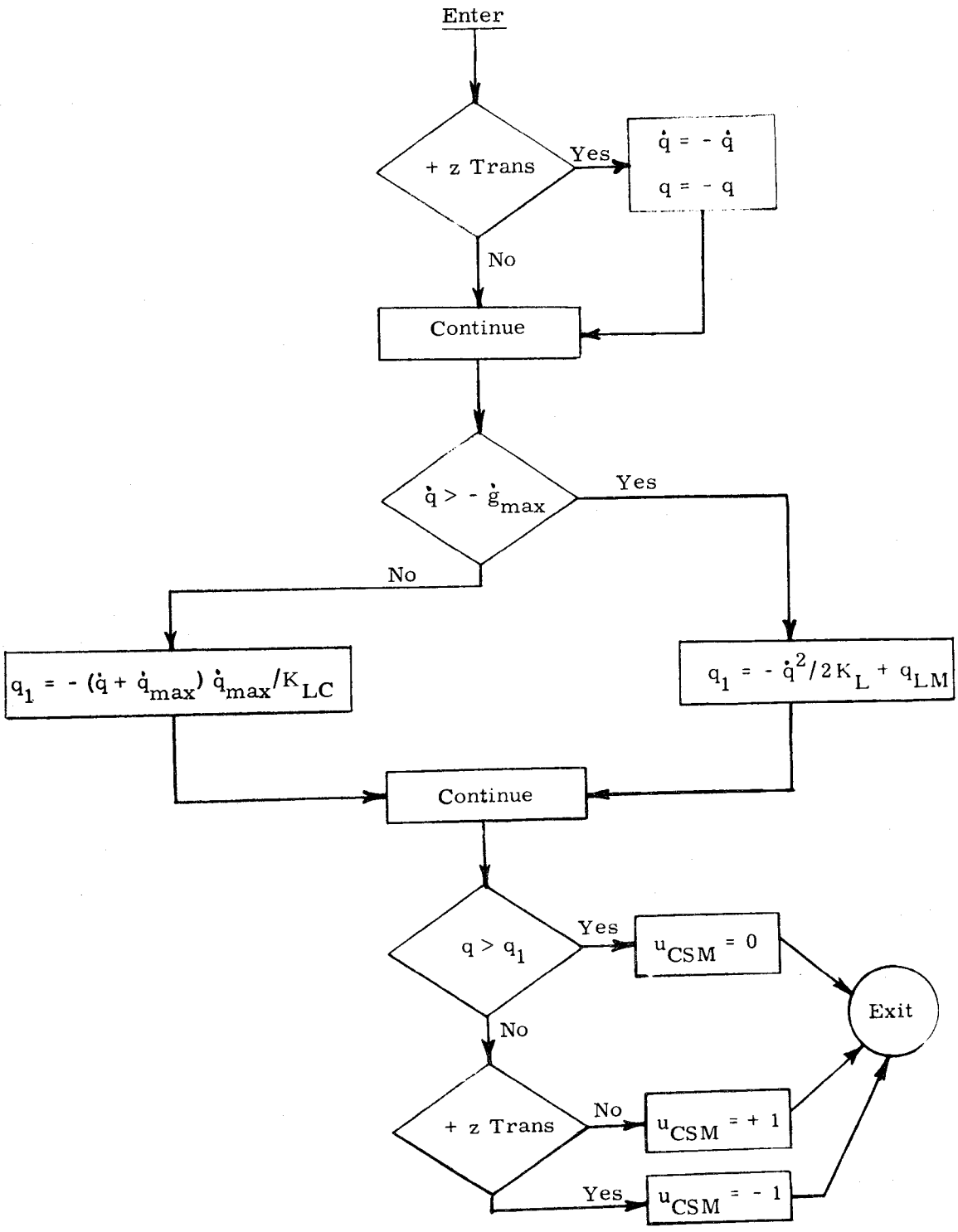

Figure 8 A Flow Chart of the Proposed Pitch Translation Attitude Hold Autopilot

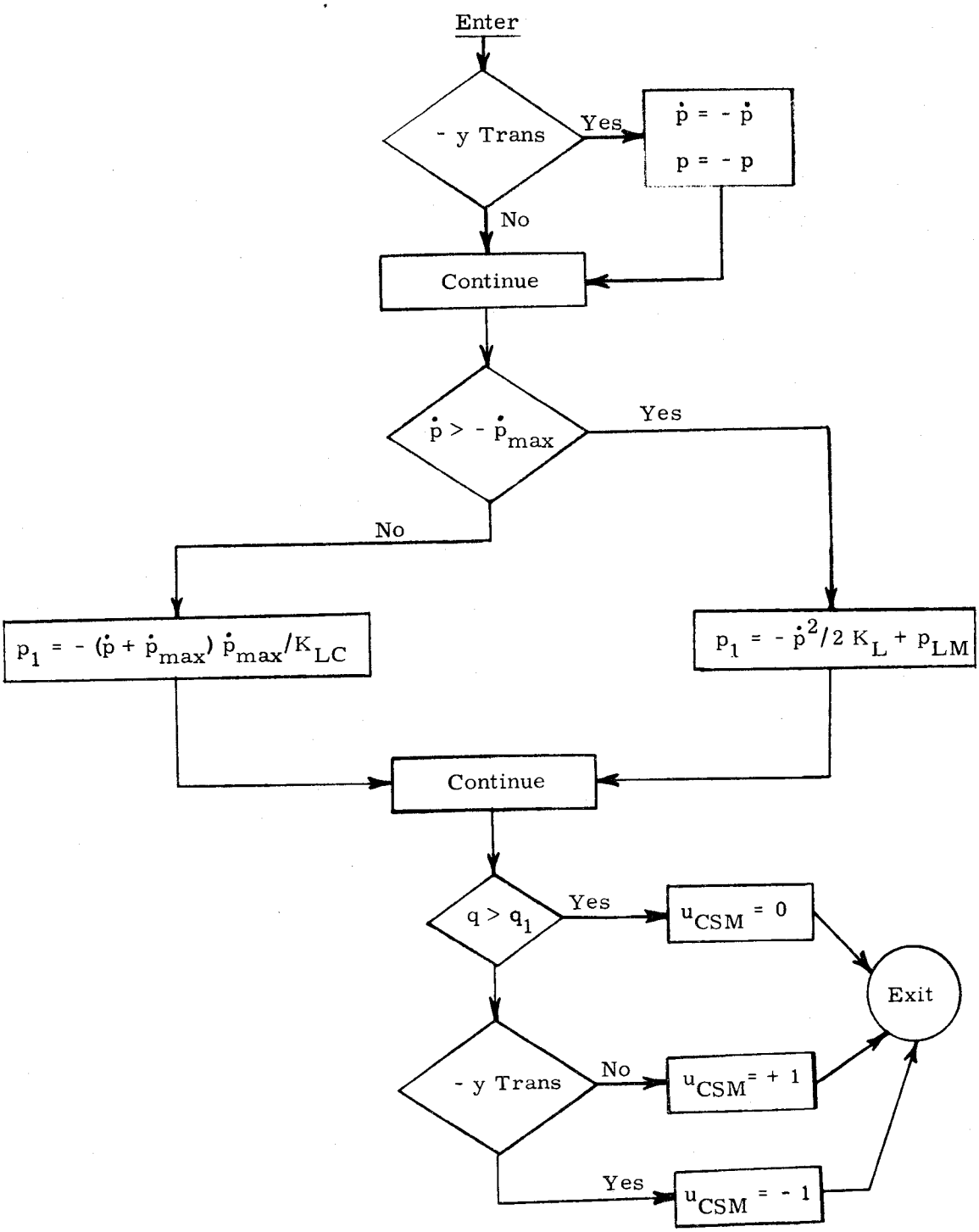

Figure 9 A Flow Chart of the Proposed Pitch Translation Attitude Hold Autopilot

Pure Attitude Hold Autopilots

For the attitude hold and maneuver modes, the pitch and yaw autopilots must be modified, so that jets # 3, 4, 7, and 8 on the CSM, and 1, 5, 9, and 13 on the LM are inhibited from firing. As was the case for the Apollo CSM and LM digital autopilots, the autopilot will be a compromise autopilot, which minimizes propellant consumption while requiring a reasonable time for a maneuver. The autopilot will drive the vehicle into a minimum impulse mode for the attitude hold.

Before presenting the proposed autopilot, a brief review of pure minimum time and pure minimum fuel autopilots is required. Again the vehicle will be considered to be a rigid body, and the rates will be assumed to be small enough so that the axes are decoupled. This means that the vehicle pitch and roll equations will be of the form

$$\ddot{x} = (TL/I)\, u = K\, u. \tag{16}$$

The well known minimum time solution for this type of system is given in Fig. 10 along with a typical trajectory.

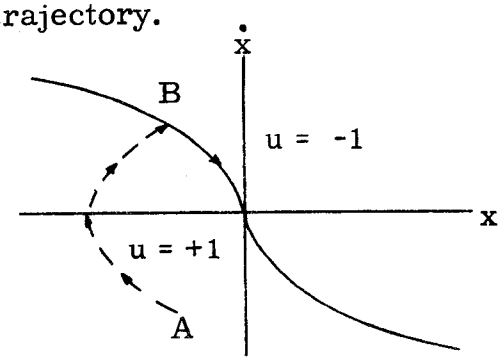

Figure 10 The Minimum Time Autopilot

The time optimal control for going from A to the origin is + 1 from A to B, and then - 1 from B to the origin. The switch curve in Fig. 10 is given by

$$x = -\dot{x}\,|\dot{x}|/2K. \tag{17}$$

A synthesis of this autopilot, suitable for a digital computer is given below.

$$\text{Key} = x + \dot{x}\,|\dot{x}|/2K$$

$$u = \begin{cases} -\,\text{sign (Key)} & \text{if Key} \neq 0 \\ -\,\text{sign}\,(\dot{x}) & \text{if Key} = 0 \end{cases}$$

For all practical purposes Key will not be zero and the autopilot can be simplified to

$$u = - \text{sign}\,(x + \dot{x}\,|\dot{x}|/2K).$$

The minimum fuel solution, similarly well known, is given in Fig. 11 along with a typical trajectory. The solid line is the switch curve and the dotted lines are typical trajectories. The optimal control is to obtain the correct sign on the velocity, coast to the parabola which passes through the origin, and follow that parabola to the origin. In order to minimize the propellant consumption, the time that the jets are on is minimized; therefore, the velocity ϵ, shown in Fig.11, approaches zero, and the time required for the maneuver approaches infinity for states which have the wrong sign on their initial velocity. A synthesis of this autopilot, suitable for a digital computer, is given below.

$$\text{Key} = x + \dot{x}\,|\dot{x}|/2K$$

$$u = \begin{cases} -\text{sign}\,(\dot{x}) & \text{if (Key } \dot{x}) > 0 \text{ or Key} = 0 \\ -\text{sign (Key)} & \text{if } \dot{x} = 0 \\ 0 & \text{if (Key } \dot{x}) < 0 \end{cases}$$

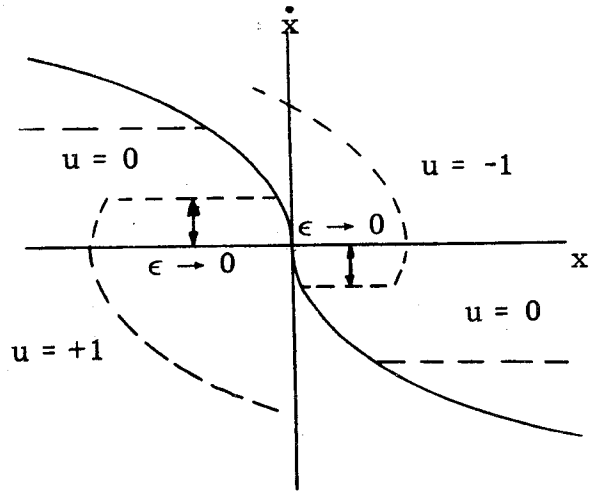

Figure 11 The Minimum Fuel Autopilot

In practice this autopilot cannot be used, because of the infinite response time required for some initial conditions. One solution is to fix the response time and then optimize the response of the system with respect to fuel. However, this solution is not very reasonable because it would require more fuel than the minimum fuel control for most sets of initial conditions that have the desired sign on the initial velocity. A more suitable and practicable autopilot is one which would vary the response time while minimizing the fuel. Just such an autopilot was proposed by Athans [1]. The response time for this autopilot will always be less than are equal to C times the minimum time, as given by the autopilot of Fig. 10, where C is a prespecified constant greater than 1, and the propellant consumption will be minimized for the given response time. The minimum fuel, minimum time compromise autopilot is shown in Fig. 12.

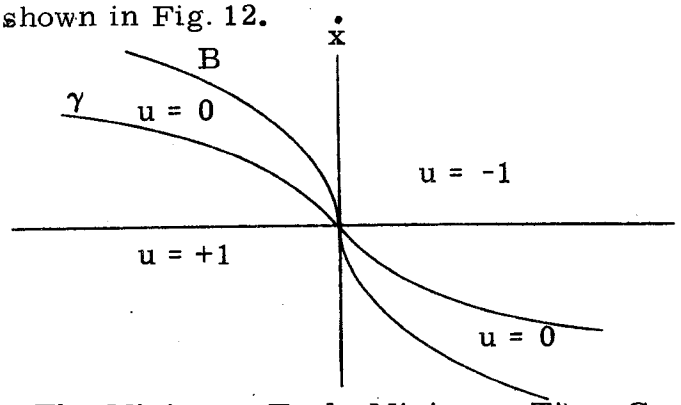

Figure 12 The Minimum Fuel, Minimum Time Compromise Autopilot

In Fig. 12, the B curve is the minimum time switching curve and is given by (17). The γ curve consists of two parabolas which define the coast region. Athans [1] showed the equation for the γ curve is:

$$x = -g\dot{x}\,|\dot{x}|\,, \tag{18}$$

where

$$g = (C/K)/(2C - 1 - 2\sqrt{C(C-1)}) - 1/2K. \tag{19}$$

Notice that as C approaches 1, (18) becomes equal to (17) and the autopilot becomes the minimum time autopilot. Similarly, as C approaches infinity, the γ curve approaches the x axis and the autopilot becomes the minimum fuel autopilot. A synthesis of the autopilot of Fig. 12, suitable for a digital computer is

$$\text{Key 1} = x + g\,\dot{x}\,|\dot{x}|$$

$$\text{Key 2} = x + \dot{x}\,|\dot{x}|/2K$$

$$u = \begin{cases} -\text{sign (Key 1)} & \text{if (Key 1 Key 2)} > 0 \\ 0 & \text{if Key 1} = 0 \\ 0 & \text{if (Key 1 Key 2)} < 0 \\ -\text{sign (x)} & \text{if Key 2} = 0 \end{cases}$$

For all practical purposes neither Key 1 or Key 2 will be zero, and the autopilot can be simplified to:

$$\text{Key 1} = x + g\,\dot{x}\,|\dot{x}|$$

$$\text{Key 2} = x + \dot{x}\,|\dot{x}|/2K$$

$$u = \begin{cases} -\text{sign (Key 1)} & \text{if (Key 1 Key 2)} > 0 \\ 0 & \text{if (Key 1 Key 2)} < 0 \end{cases}$$

In practice the object is not to bring the state of the vehicle to the origin but into a region about the origin which shall be referred to as the minimum impulse region. The minimum impulse region consists of the region where the state is close enough to the origin so that no jets are fired. The actual autopilot to be implemented is shown in Fig. 13.

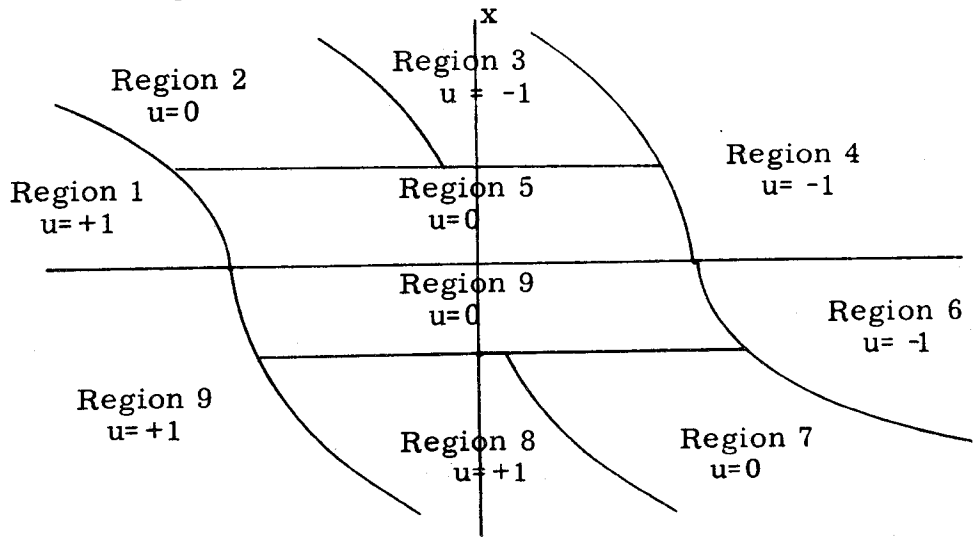

Figure 13 The Proposed Pure Attitude Hold Autopilot

In Fig. 13 the γ curve has been shifted to the edges of the attitude dead zone, and the time optimal switch curve has been given a width by adding a second parabols which is simply the time optimal switch curve shifted to the edge of the dead zone. Once the state of the vehicle is inside the minimum impulse region (regions 5 and 9), the control strategy is to allow the vehicle to coast until it reaches the edge of the dead zone, and then to fire a minimum impulse to reverse the sign of the velocity. Then the vehicle is again allowed to coast, and the procedure repeated.

In order to prevent unnecessary chattering of the jets, when the state of the vehicle is following the minimum time parabola to the minimum impulse region, the gain, K, used for the minimum time curve will be set equal to its maximum expected value.

Due to the small difference between the velocities, which define the minimum impulse region, the firing times for the jets must be calculated when the state of the vehicle is approaching the minimum impulse region. Otherwise, there is a good possibility that the state would pass through the minimum impulse region before a measurement and a subsequent estimate of the state is made. The firing times will be calculated by using (20), which can be easily derived from (16).

$$t_f = (\dot{x} + \dot{x}_{max}/2)/K, \tag{20}$$

where $\dot{x}_{max}$ is the maximum allowable magnitude of the minimum impulse made velocities. Note that in (20) the target is $(\mp \dot{x}_{max}/2)$, depending on whether or not $\dot{x}$ is $\pm$, instead of $\dot{x} = 0$.

Since the autopilot is completely symmetrical (see Fig. 11), only the upper half of the phase plane in Fig. 11 has to be programmed. When the state is in the lower half plane ($\dot{x} < 0$), -x and $-\dot{x}$ will be fed into the autopilot, and the resulting commands ($u(t)$, $u(t_f)$) will be multiplied by -1. A flow chart of the proposed autopilot is given in Fig. 14.

During a rotation maneuver this autopilot will be used with error and error rate as the input.

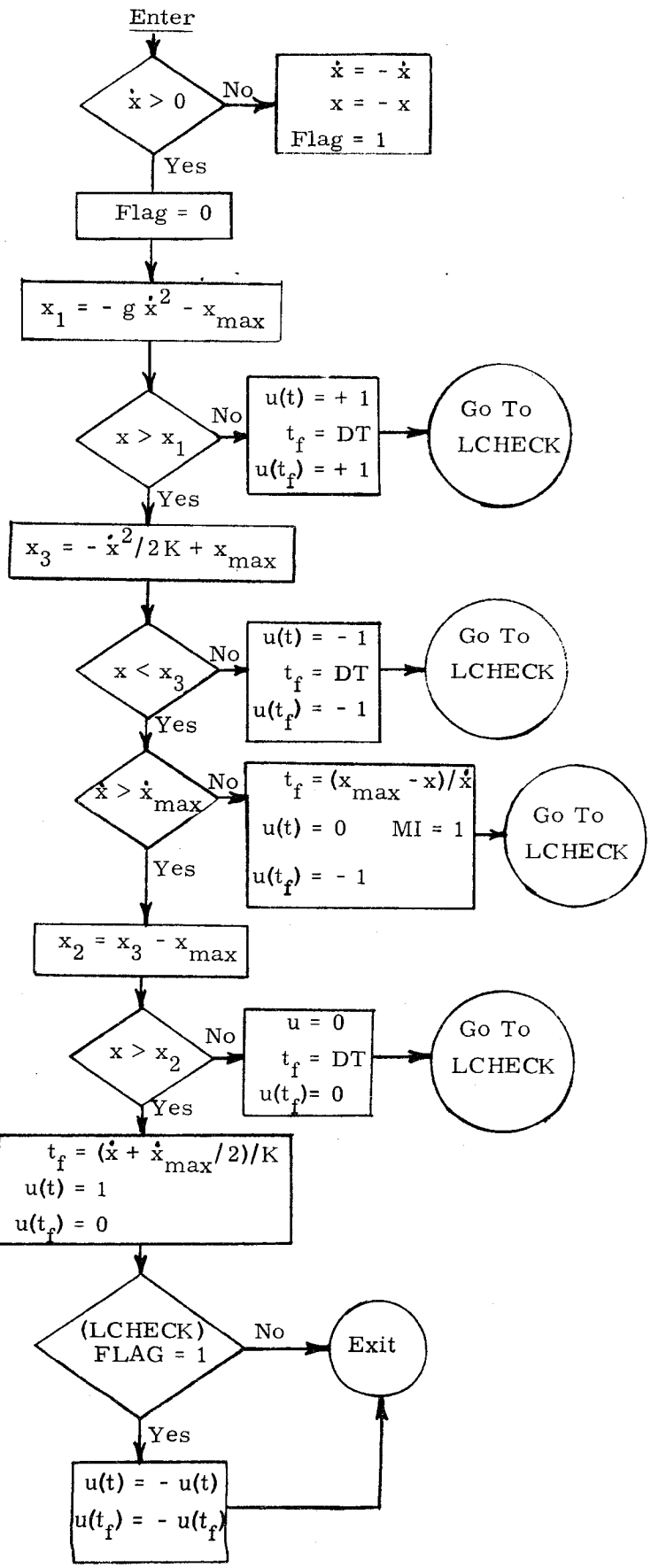

Figure 14

A Flow Chart of the Proposed Pure Attitude Hold Autopilot

Conclusions

The preliminary design of the autopilots for AAP task 2 has been completed; however, there are several problem areas remaining. To date all of the simulations with these autopilots have been with a rigid body vehicle with neither cross-axis coupling nor disturbances. Now the effects of intercoupling between axes, propellant sloshing, and body bending must be determined. In order to do this a propellant slosh model must be developed. The effects of disturbances such as gravity gradient, rotating machinery, unknown CG locations, and etc. must also be determined.

References

1. Athans, Michael, "Fuel-Optimal Control of a Double Integral Plant with Response Time Constraints," IEEE Trans. on Applications and Industry, Vol. 83, pp. 240-246, July, 1964.

2. Cherry, George and O'Connor, Joseph, "Design Principles of the Lunar Excursion Module Digital Autopilot," M. I. T. Instrumentation Laboratory Technical Report # R-499, July, 1965.

3. Crisp, R., and Keene, D., "Apollo Command and Service Module Reaction Control by the Digital Autopilot," M. I. T. Instrumentation Laboratory Technical Report # E-1964.